

Semiclassical approach to fidelity amplitude

Ignacio García-Mata,^{1,2} Raúl O. Vallejos,^{3,*} and Diego Wisniacki^{4,†}

¹*Instituto de Investigaciones Físicas de Mar del Plata (IFIMAR),
CONICET–UNMdP, Funes 3350, B7602AYL Mar del Plata, Argentina.*

²*Consejo Nacional de Investigaciones Científicas y Tecnológicas (CONICET), Argentina*

³*Centro Brasileiro de Pesquisas Físicas (CBPF), Rua Dr. Xavier Sigaud 150, 22290-180 Rio de Janeiro, Brazil*

⁴*Departamento de Física “J. J. Giambiagi”, FCEN, Universidad de Buenos Aires, 1428 Buenos Aires, Argentina*

(Dated: November 19, 2018)

The fidelity amplitude is a quantity of paramount importance in echo type experiments. We use semiclassical theory to study the average fidelity amplitude for quantum chaotic systems under external perturbation. We explain analytically two extreme cases: the random dynamics limit –attained approximately by strongly chaotic systems– and the random perturbation limit, which shows a Lyapunov decay. Numerical simulations help us bridge the gap between both extreme cases.

PACS numbers: 05.45.Mt,05.45.Pq,03.65.Sq

I. INTRODUCTION

Irreversibility in quantum mechanics cannot be explained in the same way as in classical mechanics. Instead of measuring how difficult it is to invert the individual trajectories, Peres proposed [1] as a way to understand quantum irreversibility to measure the difficulty to invert the dynamics. To put it in other words, to measure how difficult it is to implement a certain Hamiltonian or to *know* the specifics of the dynamics, given that complete isolation is impossible to attain. As a consequence the fidelity –also known as Loschmidt echo (LE) [2]– was proposed as a measure of instability of a given Hamiltonian under external perturbations. The LE is commonly defined as

$$M(t) = |O(t)|^2, \quad (1)$$

where

$$O(t) = \langle \psi_0 | e^{iH_\varepsilon t/\hbar} e^{-iH_0 t/\hbar} | \psi_0 \rangle \quad (2)$$

is the fidelity amplitude (FA) and H_0 and H_ε differ by a perturbation which is usually taken to be an additive term like $\varepsilon V(q, p)$, so ε is the perturbation strength. The importance of the LE lies not only in that it can be used to identify quantum chaos but also in that it is a measurable quantity.

There is a vast amount of work attempting to characterize the decay regimes of the LE as universal [2–5]. After a short time transient, chaotic systems decay exponentially. For small perturbation strength – Fermi Golden Rule regime – the decay rate depends quadratically on the perturbation strength. For larger perturbation the decay rate is expected to be perturbation independent, and given by the largest Lyapunov exponent of the corresponding classical system. For regular systems

the behavior is fundamentally different: for small perturbation strength the decay is Gaussian – which can in fact lead to faster decay than chaotic systems [6, 7]– and for larger values of the perturbation the decay is power law (see reviews [4, 5]). However, for chaotic systems, recent works [8–12] have reported non-universal oscillatory behavior in the decay rate of the LE as a function of the perturbation strength. In the way to elucidating the origin of such “anomalous” behavior of the LE one key quantity to understand is the FA. The FA is important in itself for a number of reasons, the most important being that in some of the echo experiments it is in fact the quantity that is measured [13–18].

It is important to remark that in previous works the characterization of decay regimes is done on the average behavior of the LE. Unlike most papers in the field – with the exception of [19] – in this work we concentrate on the average FA. The fundamental difference with [19] is that we obtain the decay regimes directly of the average FA, not requiring to compute the average fidelity. In order to do so we use the semiclassical theory known as dephasing representation (DR) [19–21]. We consider two limiting situations and obtain rigorous analytical expressions for the decay rate in both cases. In the first case we suppose the dynamics is completely random. For maps on the torus each step is given by drawing two random numbers from a uniform distribution. This corresponds to the limit of infinite Lyapunov exponent. In this limit we obtain an expression for the decay of the FA that is valid for all times – up to the saturation point. In fact it should be observed for very short times for any map – our expression is exact for $t = 1$. As the Lyapunov exponent is increased the random dynamics decay regime is observed for increasingly longer times. We have already presented related results in [22]. The other limiting case presupposes that the perturbation is completely random. That is, after each step of the map the perturbation contributes with a random phase to each trajectory. It shall be seen that this assumption can be justified in the large perturbation strength limit because semiclassical calculations involve complex exponentials of such strengths.

* vallejos@cbpf.br; <http://www.cbpf.br/~vallejos>

† wisniacki@df.uba.ar

In that case –using the DR and transfer matrix theory– we show that the asymptotic decay rate of the FA is controlled by the largest classical Lyapunov exponent λ . In other words, we are capable of predicting, analytically, the appearance of a Lyapunov regime in the average FA rather than the fidelity itself (i.e. the square of the modulus of the FA).

Even though in a realistic scenario one may not see clearly the appearance of the limiting behaviours, traces of one (or both) of them are usually present. For short times, on average the decay rate is that predicted for random dynamics. This result is valid for longer times as the dynamics becomes effectively more random –i.e. as λ grows. Then, for large perturbations, there is a crossover to an asymptotic regime where the decay rate is $\lambda/2$, independently of the perturbation. The crossover time is strongly perturbation dependent. We exhibit numerical simulations introducing a perturbation model where the amount of randomness can be varied. In this model the decay of the FA is well described by a sum of two terms, each one corresponding to one of the limiting behaviors. The relative weight of the terms depend both on λ and on the perturbation (amplitude, length scale).

The paper is organized as follows. Section II gives a brief introduction to the dephasing representation (DR). This semiclassical approximation is the basis of two analytically tractable models to be developed in the subsequent sections. The random-dynamics approach, which is valid for large Lyapunov exponents, is described in Sect. III. Using the baker-map family as a model of chaotic dynamics, and employing the transfer matrix method, we argue in Sec. IV that for large perturbations the asymptotic decay is ruled by the Lyapunov exponent.

Section V presents a brief study of mixed regimes, where the decay of the FA is bi-exponential. We show in some numerical examples that the decay rates are still given by the models mentioned above. An empirical expression for the crossover time is found.

We conclude in Sec. VI with a summary of our results and some final remarks.

II. SEMICLASSICAL DEPHASING REPRESENTATION OF THE FIDELITY AMPLITUDE

Recently [19–21] the dephasing representation was introduced to give a compact and efficient way to compute semiclassically the FA. The derivation of the DR starts by replacing the quantum propagators by the semiclassical Van Vleck propagator –this is the standard semiclassical approach. The first innovation is to use the initial value representation [23, 24] for the Van Vleck propagator. In this way a full semiclassical –so-called uniform– expression for $O(t)$ can be obtained. However, this expression is still too difficult to be computed and a further approximation is needed which involves using trajectories of H_ε with slightly different initial conditions but which remain

close to the trajectories of H_0 up to a certain time. The validity of this “dephasing trajectories” argument was justified using the shadowing theorem [19]. One of the forms of the FA obtained using the DR looks like

$$O_{\text{DR}}(t) = \int dqdp W_\psi(q, p) \exp(-i\Delta S_\varepsilon(q, p, t)/\hbar) \quad (3)$$

where $W(q, p)$ is the Wigner function of the initial state ψ and

$$\Delta S_\varepsilon(q, p, t) = -\varepsilon \int_0^t d\tau V(q(\tau), p(\tau)) \quad (4)$$

is the action difference evaluated along the unperturbed classical trajectory. In this way the decay can be attributed to the dephasing produced by the perturbation of the actions –thus the name DR. However numerics show that Eq. (3) also accounts for decay due to classical overlaps [21].

The DR is a useful tool to compute fidelity and to assess fidelity decay. Actually, when referring to fidelity decay *regimes* one refers to an average behavior. Throughout this work by average we mean average over initial states. The average FA over a number n_r of initial states is

$$\overline{O_{\text{DR}}(t)} = \frac{1}{n_r} \sum_{i=1}^{n_r} \int dqdp W_{\psi_i}(q, p) \exp(-i\Delta S_\varepsilon(q, p, t)/\hbar), \quad (5)$$

If in particular, $\{\psi_i\}_{i=0}^{n_r}$ is some complete set, the Wigner function of an incoherent sum of such a set is a constant. We then get

$$\overline{O_{\text{DR}}(t)} = \frac{1}{\mathcal{V}} \int dqdp \exp(-i\Delta S_\varepsilon(q, p, t)/\hbar), \quad (6)$$

where \mathcal{V} is the volume of phase space. This expression was used in [25] to compute the FA averaged over initial states. Henceforth we take $\mathcal{V} = 1$.

Equation (6) is the starting point of our studies. By making some additional assumptions on the dynamics and/or the perturbation we shall be able to derive analytical expressions for the decay rate of the average FA (next sections). Being at the basis of our future developments, it is necessary to be sure that (6) gives indeed an accurate description of the FA decay. The DR has successfully passed many tests in the last years [8, 21, 26], especially in quantum chemistry [27–30]. There has been a similar approach to the dephasing representation in the case of linear response functions for electronic spectra [31]. We want, though, to verify its performance in the specific systems that shall be used in this paper.

For the numerical comparisons we have preferred to use quantum maps on the torus. These maps possess all the essential ingredients of the chaotic dynamics and are, at the same time, extremely simple from a numerical point view –both at the classical and at the quantum levels. The periodic boundary conditions that the torus

geometry imposes translates in a discretization of both q and p upon quantization. The Hilbert space is then finite dimensional (dimension N) corresponding to an adimensional Planck's constant $\hbar = 1/(2\pi N)$ (we assume the torus has unit area). Position and momentum basis are related by the discrete Fourier transform (DFT). In such a setting the quantum map corresponds to a unitary operator U [32]. In particular we choose quantum maps that can be represented in the split-operator form:

$$U = e^{-i2\pi NT(\hat{p})} e^{-i2\pi NV(\hat{q})}. \quad (7)$$

The reason of using maps with this structure is twofold: (i) Many well known classical maps fall in this category, e.g., the standard map, the kicked Harper map, the sawtooth map, as well as some cat maps [32, 33]. (ii) They allow a very efficient numerical implementation due to the possibility of using the discrete Fourier transform.

The classical version of U is

$$\left. \begin{aligned} \bar{p} &= p - \frac{dV(q)}{dq} \\ \bar{q} &= q + \frac{dT(\bar{p})}{d\bar{p}} \end{aligned} \right\} \pmod{1}. \quad (8)$$

Here we shall consider the perturbed cat maps given by [34]

$$\left. \begin{aligned} \bar{p} &= p - aq + Kf(q) \\ \bar{q} &= q - b\bar{p} + \tilde{K}h(\bar{p}) \end{aligned} \right\} \pmod{1}. \quad (9)$$

In particular, for the numerics in this section and in Sec. III we consider the perturbing ‘‘forces’’

$$f(q) = 2\pi [\cos(2\pi q) - \cos(4\pi q)], \quad (10)$$

$$h(\bar{p}) = 0. \quad (11)$$

In Eq. (9) we set $K \ll 1$ and a, b such that the resulting map is completely chaotic (hyperbolic). In such a case the Lyapunov exponent is approximately

$$\lambda \approx \log \frac{1 + ab + \sqrt{ab(4 + ab)}}{2}. \quad (12)$$

Time is discrete in maps, so from now on we use the integer n to count time steps. We shall use the K -dependence of the quantum map U to define the fidelity amplitude as

$$O(n) = \langle \psi_0 | ((U_{K'}^\dagger)^n U_K^n | \psi_0 \rangle). \quad (13)$$

Accordingly, the perturbation strength is given by

$$\varepsilon = |K - K'|. \quad (14)$$

In order to calculate the semiclassical DR expression for the average FA we define a $n_s = n_q \times n_p$ grid of initial positions and momenta. Thus we get

$$\overline{O_{\text{DR}}(n)} = \frac{1}{\Omega} \sum_{q,p} \exp[-i2\pi N \Delta S_\varepsilon(q, p, n)]. \quad (15)$$

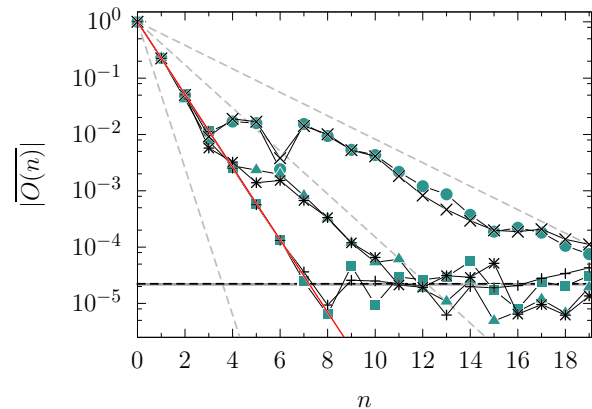


FIG. 1. (color online) Average fidelity amplitude as a function of time for the perturbed cat map of Eq. (9) for $a = b = 1$ ($\lambda = 0.96$; \bullet and \times), $a = b = 2$ ($\lambda = 1.76$; \blacktriangle and $*$) and $a = b = 20$ ($\lambda = 5.99$; \blacksquare and $+$). Both \times , $*$, and $+$ symbols correspond to the semiclassical approximation (DR) while \bullet , \blacktriangle and \blacksquare correspond to full quantum evolution. The three dashed (grey) lines represent the exponential decay $\exp(-\lambda t/2)$. The solid (red) line is $\exp(-\Gamma t)$ with Γ computed semiclassically (see Sec. III). We set $\varepsilon/\hbar = 6.433$ which corresponds to $\Gamma = 1.484$. The horizontal lines indicate saturation values: dashed (black) line is $1/\sqrt{n_s}$, with $n_s = 2 \times 10^9$ (DR); solid (grey) line is $1/\sqrt{N \times n_r}$ with $N = 2^{18}$ (Hilbert space dimension) and $n_r = 8000$ (number of initial states).

where $q = i/n_q$, $p = j/n_p$ (with $i = 0, \dots, n_q - 1$, $j = 0, \dots, n_p - 1$), and $\Omega = 1/n_q n_p$. The action difference is

$$\Delta S_\varepsilon(q, p, n) = -\varepsilon \sum_{i=1}^n F(q_i) \quad (16)$$

with $F(q) = \int f(q) dq$ and the points (q_i, p_i) are the successive iterates of the classical map of Eq. (9).

In figure 1 we show the time evolution of the fidelity amplitude, comparing the semiclassical approximation (DR) with the full quantum evolution. Three perturbed cat maps were considered (with Lyapunov exponents $\lambda = 0.96, 1.76, 5.99$) under the same perturbation. For the full quantum calculation we used a dimension $N = 2^{18}$ and averaged over $n_r = 8000$ initial coherent states. For the DR simulation the integral (6) was discretized, the total number of initial conditions being $n_s = 2 \times 10^9$.

We see that the agreement between quantum and semiclassical calculations is quite good in both cases. This makes us confident on the dephasing representation as a starting point for the analytical understanding of the average FA. In the next sections we shall describe two models that explain satisfactorily the main features observed in figure 1: for a large Lyapunov exponent the dynamics can be considered as being essentially random and the decay is single-exponential with a rate that depends only on the perturbation (Sect. III). If the Lyapunov exponent is small and/or the perturbation is large enough the

asymptotic decay rate is independent of the perturbation, equal to half the Lyapunov exponent, (Sect. IV).

To conclude this section we briefly address the matter of saturation values. The average of n_s , modulo one, complex numbers with uniform random phases goes like $1/\sqrt{n_s}$. Therefore for chaotic systems and long enough times the DR yields approximately $\overline{O_{DR}(t)} \sim 1/\sqrt{n_s}$. On the other hand, it is well known [35] that the saturation value of Eq. (13) is determined by $1/\sqrt{N}$, with N the size of the Hilbert space. Therefore in the full quantum simulation the saturation value is $\sqrt{N \times n_r}$. Notice that in the simulations we chose n_s, n_r, N so that the saturation values of both quantum and semiclassical calculations approximately coincide.

III. FIDELITY AMPLITUDE FOR RANDOM DYNAMICS

Recently [36] the DR was used to derive analytically the decay rate of the FA for perturbations acting on a small portion of phase space. The advantage of using local perturbations is that we can suppose that the trajectory becomes uncorrelated between successive hits to the perturbed region. It can be argued that the same effect can be achieved for non-local perturbations provided that λ is very large a [22].

In this section we study the behavior of $\overline{O_{DR}(n)}$ in the $\lambda \rightarrow \infty$ limit by assuming that the dynamics is purely random. This evolution is completely stochastic in the sense that there is no correlation for the different times of the evolution. To compute $\overline{O_{DR}(n)}$, we make a partition of the phase space in N_c cells. We consider that the probability to jump from cell to any other in phase space is uniform. Therefore it is straightforward to show that the mean FA results

$$\begin{aligned} \overline{O_{DR}(n)} &= \frac{1}{N_c^n} \sum_{j_1} \dots \sum_{j_n} \exp[-i(\Delta S_{\varepsilon, j_1} + \dots + \Delta S_{\varepsilon, j_n})/\hbar] \\ &= \left[\frac{1}{N_c} \sum_j \exp(-i\Delta S_{\varepsilon, j}/\hbar) \right]^n, \end{aligned} \quad (17)$$

where $\Delta S_{\varepsilon, j_k}$ is the action difference evaluated in the cell j_k at time k . The continuous limit is approached when $N_c \rightarrow \infty$. So, $\overline{O_{DR}(n)}$ results

$$\overline{O_{DR}(n)} = \left(\int \exp[-i\Delta S_{\varepsilon}(q, p)/\hbar] dq dp \right)^n, \quad (18)$$

where $\Delta S_{\varepsilon}(q, p)$ is the action difference after one step of the map. This exponential decay can be rewritten as

$$\overline{O_{DR}(n)} = \exp(-\Gamma n), \quad (19)$$

with

$$\Gamma = -\log \left| \int \exp[-i\Delta S_{\varepsilon}(q, p)/\hbar] dq dp \right|. \quad (20)$$

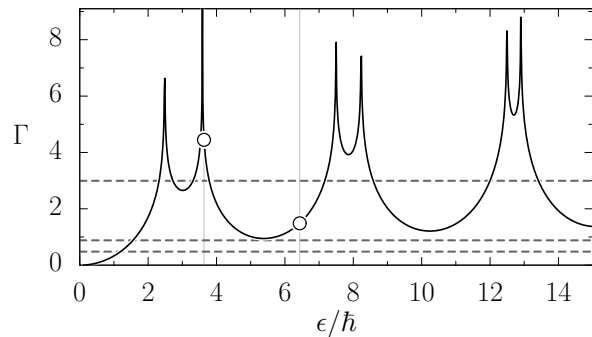


FIG. 2. (color online) Decay rate Γ computed from Eqs. (19) and (20) as a function of the rescaled perturbation. The points indicate the values chosen in figure 1 ($\varepsilon/\hbar = 6.433$) and figure 3 ($\varepsilon/\hbar = 3.635$). The dashed horizontal lines are the corresponding $\lambda/2$ used in figure 1 (0.96/2, 1.76/2 and 5.99/2).

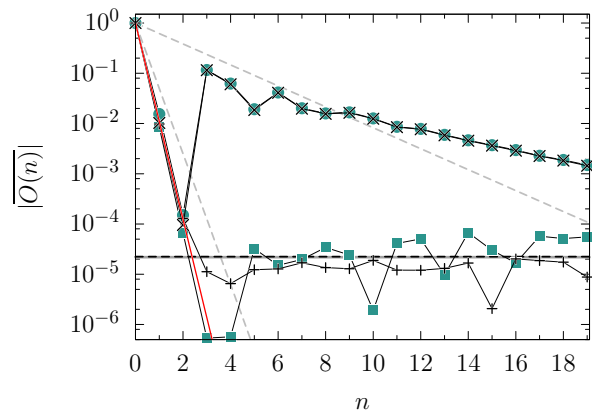


FIG. 3. (color online) Same as figure 1 with $\varepsilon/\hbar = 3.635$ corresponding to $\Gamma = 4.448$.

Equation (20) is one of the key results of this work: if the dynamics is (uncorrelated) random then the average fidelity amplitude decays exponentially with decay rate Γ . In figure 2 we plot Γ as a function of the rescaled perturbation strength ε/\hbar for the map of Eq. (9). The circles mark the perturbation strength values used in Figs. 1 and 3. Both in Figs. 1 and 3 the agreement with the random-dynamics approach is well observed for initial times. If λ is large enough ($\lambda = 5.99$ for \blacksquare and $+$ symbols in Figs. 1 and 3), the dynamics can be considered as random for practical purposes and the decay rate –up to saturation– is given by Γ . In Sec. IV we shall see in a specific deterministic model (the baker family) how a large Lyapunov exponent leads to an effective decorrelation of the successive points in a trajectory, and therefore the map behaves as if it were random.

We point out that in Figs. 1 and 3, after the initial decay following the random dynamics predictions, there is a crossover to a different decay rate. In figure 1 the second decay rate is $\lambda/2$ while in figure 3 it is not. In

Secs. IV and V we analyze in more detail this crossover behavior.

IV. THE RANDOM-PERTURBATION LIMIT

In the previous section we showed that a large Lyapunov exponent leads to a decay that is well described by the random dynamical model. Here we argue that for large enough perturbations a Lyapunov decay must be expected.

Key to our analysis is the implementation of the transfer matrix method to calculate the semiclassical average fidelity amplitude. The transfer matrix method is a standard tool in Statistical Mechanics for the calculation of the partition function of Ising lattices [37–39]. Due to the analogy between Ising partition functions (for imaginary temperature) and semiclassical periodic orbit sums, the method has also found applications in the Quantum Chaos domain [40–43].

We start by analysing the particularly simple case of the baker map and a random perturbation. Then, we provide analytical and numerical evidence showing that such a Lyapunov decay should also be observed in a larger class of chaotic maps submitted to nonrandom (large enough) perturbations.

A. The baker map and the transfer matrix method

The baker's transformation is an area preserving, piecewise-linear map of the unit square defined by [44]

$$q_1 = 2q_0 - \mu_0, \quad (21)$$

$$p_1 = (p_0 + \mu_0)/2, \quad (22)$$

where $\mu_0 = [2q_0]$, the integer part of $2q_0$. This map admits a very useful description in terms of a complete symbolic dynamics [45]. A one to one correspondence between phase space coordinates and binary sequences,

$$(p, q) \leftrightarrow \dots \mu_{-2}\mu_{-1} \cdot \mu_0\mu_1\mu_2\dots, \quad \mu_i = 0, 1, \quad (23)$$

can be constructed in such a way that the action of the map is conjugated to a shift map. The symbols are assigned as follows: μ_i is set to zero (one) when the i -th iteration of (p, q) falls to the left (right) of the line $q = 1/2$, i.e. $[2q_i] = \mu_i$. Reciprocally, given an itinerary $\dots \mu_{-2}\mu_{-1} \cdot \mu_0\mu_1\mu_2\dots$, the related phase point is obtained through the especially simple binary expansions

$$q = \sum_{i=0}^{\infty} \frac{\mu_i}{2^{i+1}} \equiv \cdot \mu_0\mu_1\dots, \quad (24)$$

$$p = \sum_{i=1}^{\infty} \frac{\mu_{-i}}{2^i} \equiv \cdot \mu_{-1}\mu_{-2}\dots \quad (25)$$

For simplicity, let us initially consider a perturbation that depends only on q . Using the binary expansions

defined above, the DR average fidelity amplitude (15,16) reads:

$$\overline{O_{\text{DR}}(n)} = \int_0^1 dq_0 e^{i\varepsilon[F(\cdot\mu_0\mu_1\mu_2\dots)+F(\cdot\mu_1\mu_2\mu_3\dots)+\dots+F(\cdot\mu_{n-1}\mu_n\mu_{n+1}\dots)]}. \quad (26)$$

Here and in the rest of this section, for the sake of a lighter notation, we write just ε in place of ε/\hbar .

In order to introduce the transfer matrix method it is necessary to truncate the binary expansions at a finite length L , i.e.,

$$q \approx \sum_{i=0}^{L-1} \frac{\mu_i}{2^{i+1}}. \quad (27)$$

Equivalently one may think that we are treating exactly a perturbation which is constant over vertical strips of equal width $1/2^L$ (we adopt this point of view). With this proviso the integral (26) becomes a finite sum:

$$\overline{O_{\text{DR}}(n)} = 2^{-(n+L-1)} \sum_{\mu_0, \dots, \mu_{n+L-2}=0,1} e^{i\varepsilon[F(\cdot\mu_0\dots\mu_{L-1})+F(\cdot\mu_1\dots\mu_L)+\dots+F(\cdot\mu_{n-1}\dots\mu_{n+L-2})]}. \quad (28)$$

The prefactor $2^{-(n+L-1)}$ represents the *area* (weight, probability) of the region in phase space corresponding to the finite symbolic string $\mu_0, \dots, \mu_{n+L-2}$ (the area depends on the length only, not on the particular code). These regions taken together form a partition of phase space into disjoint elements. All the trajectories starting in a given element have the same action.

The trick now is to express the sum above as a product of n matrices. Define the indices

$$k_0 = 2^{L-1} \times \cdot \mu_0 \dots \mu_{L-2}, \quad (29)$$

$$k_1 = 2^{L-1} \times \cdot \mu_1 \dots \mu_{L-1}, \quad (30)$$

$$\dots = \dots, \quad (31)$$

$$k_n = 2^{L-1} \times \cdot \mu_n \dots \mu_{L+n-2}. \quad (32)$$

Then we can write

$$\overline{O_{\text{DR}}(n)} = 2^{-(n/2+L-1)} \sum_{k_0, \dots, k_n} M_{k_0, k_1} M_{k_1, k_2} \dots M_{k_{n-1}, k_n}, \quad (33)$$

where the nonzero elements of the matrix M are given by

$$M_{k_0, k_1} = \frac{1}{\sqrt{2}} e^{i\varepsilon F(\cdot\mu_0\dots\mu_{L-1})} \quad (34)$$

(the convenience of having introduced a factor $\sqrt{2}$ will become clear soon). It is implicit in this definition that k_0 and k_1 must satisfy the *shift condition*, i.e., they must share the bits $\mu_1 \dots \mu_{L-2}$ [see Eqs. (29,30)], otherwise the matrix element is set to zero. The shift condition determines that nonzero elements are located on two staircases of slope $1/2$ (“baker structure”), explicitly given by

$$k_1 = 2k_0 - 2^{L-1}\mu_0 + \mu_{L-2} \quad (35)$$

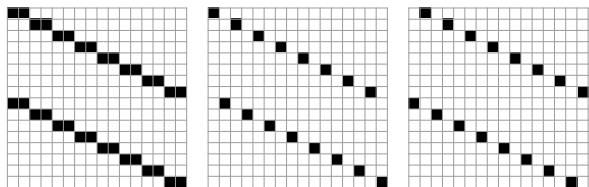


FIG. 4. The transfer matrix M (left) can be split into two unitary matrices U_1, U_2 (center, right). Nonzero elements are shown as black squares ($L = 5$, schematic).

(see figure 4).

If one defines the unit-norm vector

$$|1\rangle = \frac{1}{\sqrt{2^{L-1}}}(1, 1, \dots, 1), \quad (36)$$

then Eq. (33) can be written in the compact way

$$\overline{O_{\text{DR}}(n)} = 2^{-n/2} \langle 1 | M^n | 1 \rangle. \quad (37)$$

This is a remarkable result: the decay properties of the average fidelity amplitude are embodied in the spectrum of a finite matrix. In particular, the asymptotic decay is ruled by the largest eigenvalue (in modulus) of M . The special staircase structure of the transfer matrix allows us to deduce some general properties of its spectrum.

For a fine discretization, the phase in Eq. (34) varies by small jumps along the staircases of M , the size of the jumps depending both on the characteristic spatial scale of $F(q)$ (“correlation length”) and on the perturbation amplitude ε . As the correlation length decreases and/or the amplitude grows, neighboring matrix elements become increasingly decorrelated. This leads us to consider, as a reference, an ensemble of random transfer matrices having the same structure as M , but whose phases are i.i.d. random variables chosen from a uniform distribution in $[0, 2\pi]$.

Random or not, because of its particular structure, the matrix M can be split as a sum of two unitary matrices U_1, U_2 (see figure 4):

$$M = \frac{1}{\sqrt{2}}(U_1 + U_2). \quad (38)$$

When U_1 and U_2 are random unitary matrices drawn independently from the Circular Unitary Ensemble (CUE) [32, 46], analytical and numerical studies say that the spectrum of M lies almost entirely inside the unit circle in the complex plane. As the dimension of U_i is increased, the largest eigenvalue (in modulus) tends to the unit circle. In the limit of infinite dimensional matrices, all the spectrum is contained in the unit disk [43, 47].

We have not attempted an analytical study of the spectral properties of random matrices with the baker structure. However, our numerical calculations show that they possess very similar statistical properties to those of the

normalized sum of two CUE matrices (as far as the spectrum close to the unit circle is concerned). Figure 5 shows clearly that most eigenvalues are distributed inside the unit circle, the relative number of “outsiders” decreasing as dimension is increased.

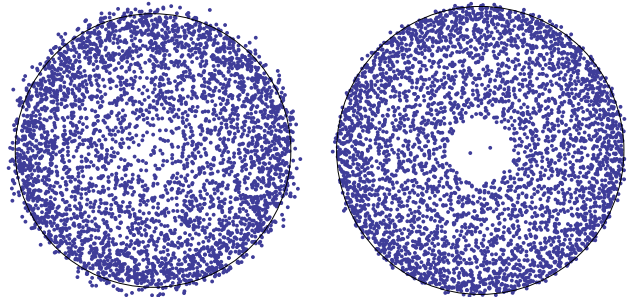


FIG. 5. (Color online) Eigenvalues z_i of random matrices having the baker structure. Shown are the combined spectra of 64/8 matrices of dimension $64 \times 64/512 \times 512$ (left/right). Circles of unit radii were drawn for reference.

So, as the leading eigenvalues of M are close to the unit circle, we conclude that for a random perturbation the asymptotic decay of $\overline{O_{\text{DR}}(n)}$ is governed by the prefactor in (37), thus we have

$$|\overline{O_{\text{DR}}(n)}|^2 \sim 2^{-n}. \quad (39)$$

This is an exponential decay, with a rate given by the Lyapunov exponent of the baker map. This is the other key result of the present work: starting from the FA, and using the DR and the transfer matrix method we obtain that the asymptotic decay of the average FA is given by $\lambda/2$ (consequently the fidelity decays with the rate lambda).

After having analysed the random transfer-matrix model, we question to what extent a nonrandom perturbation may lead to a random-matrix behavior. As mentioned before, e.g., a smooth but large perturbation may cause a randomization of the phases (34). In order to check this expectation we consider now the baker dynamics with the action difference of Eqs. (16,10), i.e., $F(q) = \sin(2\pi q) - \sin(4\pi q)/2$. The spectrum of the corresponding $M(\varepsilon)$ is shown in figure 6. There we see that for, say, $\varepsilon > 10$ the leading eigenvalues settle down in a small neighborhood of the unit circle. Then, for such large perturbations $|\overline{O_{\text{DR}}(n)}|^2$ decays with a rate which is close to the Lyapunov exponent of the classical map.

Note, however, that in typical numerical simulations the decay rate may exhibit some departure from the Lyapunov exponent. This may be due to two reasons. First, the perturbation amplitude may be not large enough for the settling down of the Lyapunov regime. Second, even for completely random perturbations, if M is finite-dimensional then the leading eigenvalue will be in general outside the unit circle. It is true that, as the dimension N of M is increased, the leading eigenvalue tends to the

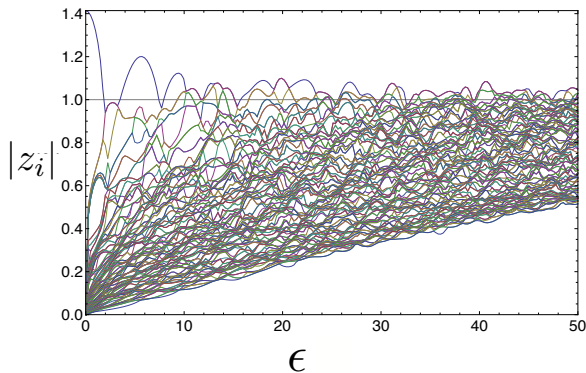


FIG. 6. (Color online) Transfer matrix eigenvalues (moduli) as a function of perturbation amplitude. The perturbation $F(q) = \sin(2\pi q) - \sin(4\pi q)/2$ was discretized in a lattice of 256 points ($L = 7$).

unit circle, but it does so very slowly, possibly like $N^{-1/3}$ [43]. So, in practice, some finite deviations from the Lyapunov decay rate should not be ruled out.

B. Extensions

Here we present some extensions of the application of the transfer matrix method to account for more general maps and/or perturbations.

First note that perturbations that depend both on q and p can easily be accommodated in the transfer-matrix scheme, for, according to (23), it requires only adding some symbols for the discretization in p .

Now consider the B -adic baker map defined by ([48])

$$q_1 = Bq_0 - \nu_0, \quad (40)$$

$$p_1 = (p_0 + \nu_0)/B, \quad (41)$$

where B is an integer ≥ 2 , and $\nu = 0, 1, \dots, B-1$. This map is completely analogous to the usual ($B = 2$) baker map, but with expansion rate B . At the symbolic level it corresponds to a full shift on B symbols [45]. Its Lyapunov exponent is $\log B$. Thus, by making B large enough we shall be able to enter the random-dynamics regime (Sect. III).

The transfer matrix M is constructed in a similar way as we did for the baker: basically, all we have to do is to change from base-2 to base- B in the standard-baker formulas. By making the appropriate substitutions, and skipping the details, one arrives at the following expression for the average FA

$$\overline{O_B(n)} = B^{-n/2} \langle 1 | M_B^n | 1 \rangle, \quad (42)$$

with $|1\rangle$ a unit-norm vector of length B^{L-1} .

For a perturbation that only depends on q the non-null elements of M_B read

$$(M_B)_{k_0, k_1} = \frac{1}{\sqrt{B}} e^{i\varepsilon F(\nu_0 \dots \nu_{L-1})}, \quad (43)$$

where ν_i are the “decimal” digits of the B -ary expansion of the coordinate q , truncated at depth L . The non-null elements of M_B lie along B flights of stairs of slope $1/B$ (riser=1, tread= B). In analogy to the $B = 2$ case, we can split M_B into a sum of unitary matrices:

$$M_B = \frac{1}{\sqrt{B}} \sum_{i=1}^B U_i. \quad (44)$$

Again, in the case that U_i are large independent CUE matrices, it is possible to show that the spectrum of M_B is almost completely contained in the unit disk in the complex plane [47]. The same behavior is expected for the transfer matrix of the baker family, when a nonrandom but large enough perturbation is considered. In such a case, one would have the asymptotic decay

$$\overline{O_B(n)} \sim e^{-\lambda_B n/2}, \quad (45)$$

with $\lambda_B = \log B$, the Lyapunov exponent of the classical B -baker map. As an example, we show in figure 7 the transfer matrix spectrum for $B = 13$ and a smooth perturbation. Plot are the decay rates

$$\gamma_i = \frac{\log B}{2} - \log |z_i|, \quad (46)$$

where $\{z_i\}$ stand for the eigenvalues of M_B .

Focusing on the asymptotic decay, we see that for small perturbation amplitudes the decay is very well described by random-dynamical model, as was expected from the discussion of Sect. III. Note, however, that the extension of the random-dynamic regime is sensitive to the *form* of the perturbation. For large ε the leading decay rate fluctuates around the Lyapunov value $(\log B)/2$, in a similar way as we had seen in the case of the standard baker.

The baker family permits a transparent estimation of the crossover point between random-dynamics and Lyapunov regimes. For a q -dependent perturbation and a B -baker map, the average fidelity amplitude is given by

$$\overline{O_{DR}(n)} = \int_0^1 dq_0 e^{i\varepsilon[F(q_0)+F(q_1)+\dots+F(q_{n-1})]}. \quad (47)$$

Here it is implicit that q_1, q_2, \dots are related to q_0 by the dynamics. Alternatively we can take the q_i to be independent and write

$$\overline{O_{DR}(n)} = \int dq_0 dq_1 \dots dq_{n-1} e^{i\varepsilon[F(q_0)+F(q_1)+\dots+F(q_{n-1})]} \times P(q_0, q_1, \dots, q_{n-1}), \quad (48)$$

where

$$P(\dots) = \delta(q_1 - g(q_0)) \delta(q_2 - g^2(q_0)) \dots \delta(q_{n-1} - g^{n-1}(q_0)), \quad (49)$$

and $g(q) = Bq - [Bq]$.

If the joint probability distribution P were factorable, then we would recover the formula for random dynamics. Strictly speaking this factorization is impossible for a

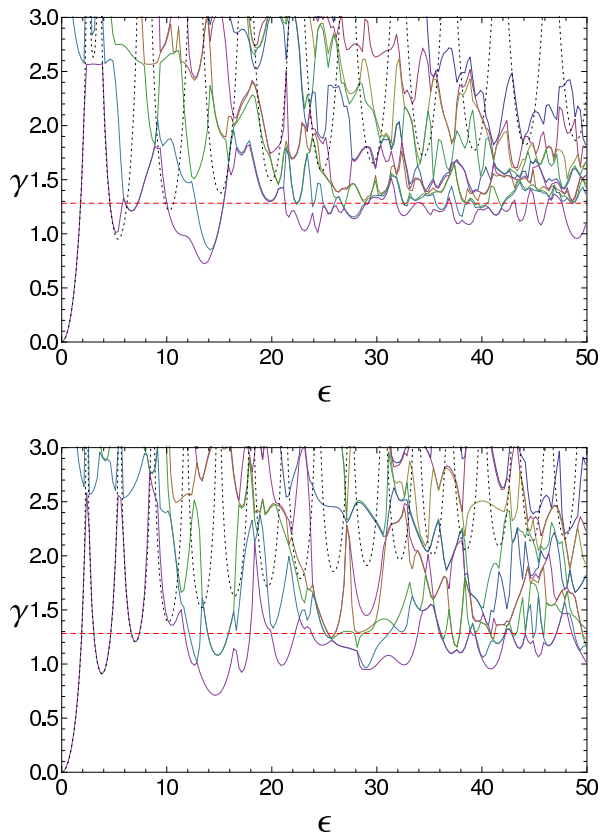


FIG. 7. (Color online) Transfer matrix decay rates for the $B = 13$ baker as a function of perturbation amplitude. We considered two perturbed actions $F(q) = \sin(2\pi q) - \sin(4\pi q)/2$ (top panel) and $F(q) = \sin(2\pi q)$ (bottom panel). These functions were discretized in a lattice of 2197 points ($L = 3$). Dashed horizontal lines correspond to Lyapunov decay, i.e., $(\log B)/2$. Dotted lines are the predictions of the random-dynamics model.

deterministic dynamics, however, when considering P in the context of the integral above one sees that P admits some coarse graining without affecting the integral. This is true whenever the scale for the smoothing is smaller than the typical scale of variation of the phase $\exp(i\varepsilon \dots)$, which is of the order of $1/\varepsilon$. The smaller ε , the larger the smoothing of P we are allowed to do. Suppose that the smoothing consists of substituting P by a histogram of bin size $a \sim 1/\varepsilon$ for each coordinate (see figure 8). Then, by choosing $a \geq 1/B$ the smoothed distribution becomes a constant, i.e., becomes separable (the marginals are constant). We conclude that for $\varepsilon \lesssim B$ the distribution P is *effectively* separable and the random-dynamic result is applicable.

Concerning the application of the transfer matrix method to more general maps with a finite symbolic dynamics, e.g., cat maps, it is likely that the scheme can also be adapted to this case. The general structure of the transfer matrix will be the same as that of the corresponding baker with the same number of symbols. The

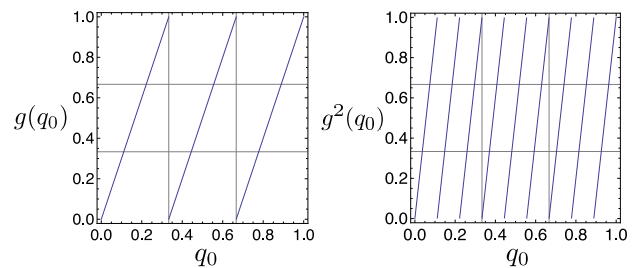


FIG. 8. The probability distribution is a product of delta functions $\delta(q_1 - g(q_0))\delta(q_2 - g^2(q_0)) \dots$. Gridlines define the critical square binning. All bins contain the same probability, meaning that the histogram is constant, therefore separable. The same is true for any bin size larger than $1/B$ ($B = 3$ in these plots).

novelty is that some zeros will appear along the staircases whenever the associated symbolic sequence is prohibited (the information about allowed and prohibited sequences is contained in the transition matrix [45]). The correspondence between symbols and phase space points will be nontrivial, but it could be settled numerically, just by launching initial conditions and registering the sequence of Markov regions that are visited.

The main obstacle we see at the moment is that in general the symbolic sequences do not have the same weight. It is possible that these weights can be embodied in the transfer matrix, or it may be a good approximation to assume that for long sequences the weights are equal. This issue, which exceeds the original scope of the present paper, is currently being investigated [49].

V. CROSSOVER REGIME

In the previous sections we provided analytical descriptions of the FA in two extreme cases: the random dynamics limit and the random perturbation limit. The first model provides a satisfactory description for initial times in general and for all times – before saturation – in the large λ limit (ideally $\lambda \rightarrow \infty$). The second explains the appearance of the Lyapunov regime for long times and large enough perturbations.

In many cases the time behavior of the FA is not pure, but shows a crossover from a random-dynamics decay (short times) to a random-perturbation decay (long times). We know that for short times the influence of the dynamics is not significant on average, then the trajectories in the DR formula (15) behave like random walks with uncorrelated jumps. Therefore, for short times the decay of the average fidelity amplitude is given by Eq. (20) –it is exact for $t = 1$. In addition, for a general smooth perturbation with large amplitude, we have shown that there is a randomization of phases yielding an effectively random perturbation. As a consequence, the well known Lyapunov decay emerges in the large ε limit.

There remains a need for understanding the crossover (in the time domain) between random-dynamics and Lyapunov decays.

In order to investigate the crossover we resorted to numerical simulations using the DR and the cat map (9) with a random perturbation. We divided the torus into $N_c \times N_c$ square cells, assigning a random constant value $v_i \in [-0.5, 0.5]$ to each cell, with $i \in [1, N_c^2]$. Next we computed $\overline{O_{\text{DR}}(n)}$ by summing over n_s initial conditions and then averaged $|\overline{O_{\text{DR}}(n)}|$ over N_{rc} realizations of the perturbation.

In figure 9 we show the results of our simulations for various values of ϵ and λ . Using Eqs. (19) and (20) we computed the decay rate Γ for the initial times (see inset). We can already see on the top panel that $\langle |\overline{O_{\text{DR}}(n)}| \rangle$ has three well defined regimes: two exponential decays followed by the expected saturation due to finite number of initial conditions. Then, up to the saturation point, the decay is well described by

$$\langle |\overline{O_{\text{DR}}(n)}| \rangle \sim \exp(-\Gamma n) + A \exp(-\lambda n/2). \quad (50)$$

We found empirically that, in our particular model, the prefactor A is given by

$$A = \lambda/N_c. \quad (51)$$

So, when $\lambda \rightarrow \infty$ the dynamics is random, the second term vanishes, and the decay rate is Γ for all times before saturation, as predicted in Sec. III. When λ is finite but the perturbation is completely random ($N_c \rightarrow \infty$) the first term in Eq. (50) dominates the initial decay. The reason for this is that deterministic motion together with random perturbations looks, on short time scales, like random dynamics (as far as the accumulation of phases is concerned).

In figure 9 (top and middle panels) the dependence of A with λ is clearly observed. The dependence with N_c is established in the bottom panel, where we plot $\langle |\overline{O_{\text{DR}}(n)}| \rangle$ for three different orders of magnitude of the randomness parameter N_c . We remark that, as expected, the crossover point depends both on the dynamics (through λ) and on the perturbation (through N_c). We can clearly see this in the middle panel of figure 9 where we show $\langle |\overline{O_{\text{DR}}(n)}| \rangle$ for different values of the rescaled perturbation strength ϵ/\hbar [and for $\lambda = 0.96$, corresponding to $a = b = 1$ in Eq. (9)] and in the bottom panel of the same figure where we plot $\langle |\overline{O_{\text{DR}}(n)}| \rangle$ for one value of ϵ/\hbar and $N_c = 10, 100$ and 1000 . We can again see that Eq. (50) describes quite well the decay up to the saturation value.

We thus verify that the crossover regime can be described by a natural bi-exponential law combining the random-dynamic and Lyapunov decays.

VI. CONCLUSIONS

We have analyzed the average fidelity amplitude, a quantity that characterizes the instability and irre-

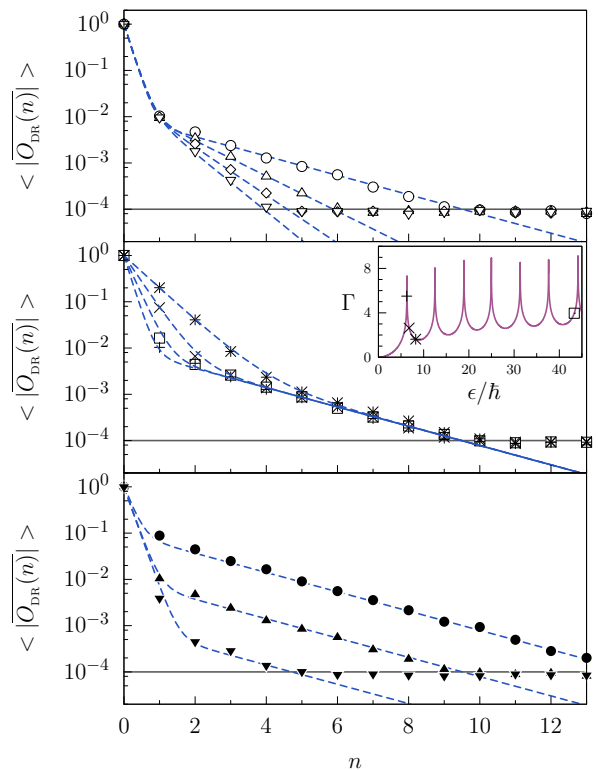


FIG. 9. (color online) Top: $\langle |\overline{O_{\text{DR}}(n)}| \rangle$ for $\epsilon/\hbar = 6.2589$ (+ symbol in the inset), and different values $a = b = 1, 2, 3$ and 4 in Eq. (9) giving $(\circ) \lambda = 0.96$, $(\triangle) \lambda = 1.76$, $(\diamond) \lambda = 2.389$ and $(\nabla) \lambda = 2.887$ respectively. Middle: $\langle |\overline{O_{\text{DR}}(n)}| \rangle$ for $a = b = 1, \lambda = 0.96$ and different perturbation strengths: (+) $\epsilon/\hbar = 6.2589$; (\times) $\epsilon/\hbar = 6.794$; ($*$) $\epsilon/\hbar = 8.235$; (\square) $\epsilon/\hbar = 43.318$. Inset: $\Gamma(t)$ computed from $N_{\text{rc}} = 100$ realizations of the perturbation with $N_c = 100$. The points indicate the value of ϵ/\hbar for the curve with corresponding symbol on the bottom panel. Bottom: $\langle |\overline{O_{\text{DR}}(n)}| \rangle$ for $\epsilon/\hbar = 6.2589$ (+ symbol in the inset), for three different values of N_c : (\bullet) $N_c = 10$, (\blacktriangle) $N_c = 100$ and (\blacktriangledown) $N_c = 1000$ ($a = b = 1, \lambda = 0.96$). The dashed blue line (in all panels) corresponds to the bi-exponential in Eq. (50). The horizontal gray lines correspond to the expected saturation values.

versibility of perturbed quantum evolution. We have taken as a starting point a well established semiclassical theory – the dephasing representation. Our first key result is obtained in the limit of random dynamics. We show that in that case the decay of the average FA is exponential for all times – up to the saturation – and we give an analytic expression for the corresponding decay rate. Maps on the torus with a very large Lyapunov exponent are expected to mimic random dynamics rather precisely. Thus the decay rate Γ obtained in equation (20) is to be observed for increasingly larger periods of time as λ is increased. Numerical results shown in figures 1 and 3 confirm this assertion.

Our second key result is that using the DR and a novel approach in this context – the transfer matrix method – we were able to predict that the asymptotic decay of the

average fidelity amplitude should be perturbation independent and given by $\lambda/2$. We are even able to explain possible deviations from this behavior. We point out that the Lyapunov, as well as other regimes were obtained in [19] analyzing statistics of action differences in an expression which is obtained from the square of the average FA (equation (6)). However in that article the short time behavior due to random dynamics-like behavior is not observed. In addition, one major advantage of our approach is that we do not need to sum over pairs of trajectories – a difficulty that arises in the squaring needed to perform average fidelity studies.

As consequence, we have both analytical and numerical evidence to conclude that the average FA for an arbitrary chaotic map, should decay initially with a decay rate given by the random dynamics approximation, and for long times there is the Lyapunov regime. We cannot yet predict in a generic case the behavior or the time where the crossover takes place. Nevertheless in an attempt to understand this problem we have studied a model of random perturbations which helped us in determining that for random perturbations and intermediate times the decay is also given by the Lyapunov exponent.

In [22] it is shown that the decay of Loschmidt echo has three regimes as a function of the perturbation strength. The well known –quadratic– Fermi golden rule regime

is valid for small perturbations. Then there is a regime where the decay rate is given by Γ (computed for random dynamics) and after that there is a crossover to a perturbation independent regime given by the Lyapunov exponent λ . We believe that this paper is an important step towards understanding this complex behavior of the LE. We remark that the average FA is tightly related to the LE but has some fundamental differences. In fact, if we suppose that n_s is the number of initial conditions then the average LE can be expressed as a sum of the square of the average of the FA (times n_s) minus a sum of “nondiagonal” terms consisting of products of $O(t)$ for different initial conditions. Here we have taken a significant step forward by understanding one of the parts of the LE: the average FA, which is in itself an important quantity in many experiments. In order to fully comprehend the behavior of the LE further work is needed [49].

ACKNOWLEDGMENTS

We are grateful to F. Toscano for useful suggestions. We received partial support from ANCyPT (grant PICT-2010-1556), UBACyT (grant X237) (Argentina), CNPq (Brazil), and UNAM-PAPIIT (grant IN117310) (Mexico).

-
- [1] A. Peres, Phys. Rev. A **30**, 1610 (1984).
 - [2] R. A. Jalabert and H. M. Pastawski, Phys. Rev. Lett. **86**, 2490 (2001).
 - [3] Ph. Jacquod, P. G. Silvestrov, and C. W. J. Beenakker, Phys. Rev. E **64**, 055203 (2001).
 - [4] T. Gorin, T. Prosen, T. Seligman, and M. Žnidarič, Phys. Rep. **435**, 33 (2006).
 - [5] Ph. Jacquod and C. Petitjean, Adv. Phys. **58**, 67 (2009).
 - [6] T. Prosen and M. Žnidarič, J. Phys. A: Math. Gen. **35**, 1455 (2002).
 - [7] T. Prosen, Phys. Rev. E **65**, 036208 (2002).
 - [8] W. Wang, G. Casati, and B. Li, Phys. Rev. E **69**, 025201 (2004).
 - [9] M. Andersen, A. Kaplan, T. Grünzweig, and N. Davidson, Phys. Rev. Lett. **97**, 104102 (2006).
 - [10] E. N. Pozzo and D. Domínguez, Phys. Rev. Lett. **98**, 057006 (2007).
 - [11] N. Ares and D. A. Wisniacki, Phys. Rev. E **80**, 046216 (2009).
 - [12] B. Casabone, I. García-Mata, and D. Wisniacki, Europhys. Lett. **89**, 50009 (2010).
 - [13] O. I. Lobkis and R. L. Weaver, Phys. Rev. Lett. **90**, 254302 (2003).
 - [14] R. Schäfer, H.-J. Stöckmann, T. Gorin, and T. H. Seligman, Phys. Rev. Lett. **95**, 184102 (2005).
 - [15] R. Schäfer, T. Gorin, T. H. Seligman, and H.-J. Stöckmann, New J. Phys. **7**, 152 (2005).
 - [16] T. Gorin, T. H. Seligman, and R. L. Weaver, Phys. Rev. E **73**, 015202 (2006).
 - [17] O. I. Lobkis and R. L. Weaver, Phys. Rev. E **78**, 066212 (2008).
 - [18] B. Köber, U. Kuhl, H.-J. Stöckmann, T. Gorin, D. V. Savin, and T. H. Seligman, Phys. Rev. E **82**, 036207 (2010).
 - [19] J. Vaníček, Phys. Rev. E **70**, 055201 (2004).
 - [20] J. Vaníček and E. J. Heller, Phys. Rev. E **68**, 056208 (2003).
 - [21] J. Vaníček, Phys. Rev. E **73**, 046204 (2006).
 - [22] I. García-Mata and D. A. Wisniacki, J. Phys. A: Math. Theor. **44**, 315101 (2011).
 - [23] W. H. Miller, J. Chem. Phys. **53**, 3578 (1970).
 - [24] W. H. Miller, J. Phys. Chem **105**, 2942 (2001).
 - [25] J. Vaníček, (2004), arXiv:arXiv:quant-ph/0410205.
 - [26] W. Wang, G. Casati, B. Li, and T. Prosen, Phys. Rev. E **71**, 037202 (2005).
 - [27] B. Li, C. Mollica, and J. Vaníček, J. Chem. Phys. **131**, 041101 (2009).
 - [28] T. Zimmermann and J. Vaníček, J. Chem. Phys. **132**, 241101 (2010).
 - [29] T. Zimmermann, J. Ruppen, B. Li, and J. Vaníček, Int. J. Quant. Chem. **110**, 2426 (2010).
 - [30] M. Wehrle, M. Šulc, and J. Vaníček, CHIMIA International Journal for Chemistry **65**, 334 (2011).
 - [31] Q. Shi and E. Geva, J. Chem. Phys. **122**, 064506 (2005).
 - [32] F. Haake, *Quantum Signatures of Chaos* (Springer-Verlag, Berlin, 2010).
 - [33] A. M. O. de Almeida, (Cambridge University Press, Cambridge, UK, 1988).

- [34] M. B. de Matos and A. M. O. de Almeida, *Ann. Phys.* **237**, 46 (1995).
- [35] M. Gutiérrez and A. Goussev, *Phys. Rev. E* **79**, 046211 (2009).
- [36] A. Goussev, D. Waltner, K. Richter, and R. A. Jalabert, *New J. Phys.* **10**, 093010 (2008).
- [37] J. F. Dobson, *J. Math. Phys.* **10**, 40 (1969).
- [38] C. Borzi, G. Ord, and J. K. Percus, *J. Stat. Phys.* **46**, 51 (1987).
- [39] L. E. Reichl, *A Modern Course in Statistical Physics* (John Wiley & Sons, Inc., New York, 1998).
- [40] M. C. Gutzwiller, *Chaos in Classical and Quantum Mechanics* (Springer, New York, 1990).
- [41] L. Kaplan and E. J. Heller, *Phys. Rev. Lett.* **76**, 1453 (1996).
- [42] U. Smilansky and B. Verdene, *J. Phys. A: Math. Gen.* **36**, 3525 (2003).
- [43] G. G. Carlo, R. O. Vallejos, and R. F. Abreu, *Phys. Rev. E* **82**, 046220 (2010).
- [44] V. I. Arnold and A. Avez, *Ergodic Problems in Classical Mechanics* (Addison-Wesley, Reading, 1989).
- [45] R. L. Adler, *Bull. Am. Math. Soc.* **35**, 1 (1998).
- [46] M. L. Mehta, *Random Matrices* (Elsevier, Amsterdam, 2004).
- [47] A. Görlich and A. Jarosz, (2004), arXiv:arXiv:math-ph/0408019.
- [48] M. M. Sano, *CHAOS* **10**, 195 (2000).
- [49] I. García-Mata, R. O. Vallejos, and D. A. Wisniacki, In preparation.